

INKJET-PRINTING OF PHOSPHORUS AND BORON DOPANT SOURCES FOR TUNNEL OXIDE PASSIVATING CONTACTS

Z. Kiaee, C. Reichel, R. Keding, M. Nazarzadeh, R. Lohmann, F. Feldmann, M. Jahn, J. D. Huyeng, M. Hermle, F. Clement

Fraunhofer Institute for Solar Energy Systems (ISE), Heidenhofstr. 2, 79110 Freiburg, Germany
Phone: +49 761 - 4588 5654; e-mail: zohreh.kiaee@ise.fraunhofer.de

ABSTRACT: This paper presents inkjet-printing of phosphorus and boron dopant inks for the formation of tunnel oxide passivating contacts (TOPCon) for back-contact back-junction (BC-BJ) silicon solar cells. The successful realization of passivating contacts utilizing printing technologies is a crucial prerequisite to simplify the fabrication process of BC-BJ cells while approaching the theoretical efficiency limit of silicon solar cells. In this work, the focus is set on developing inkjet printing processes for the application of dopant sources towards higher precision, homogeneity of printed lines and lifetime, in order to establish high passivation quality for TOPCon. Excellent passivation quality is achieved for inkjet-printed *n*-type (phosphorus) poly-Si surfaces with an implied open-circuit voltage iV_{OC} of up to 733 mV and an implied fill factor iFF of up to 86.4%. For *p*-type (boron) poly-Si, iV_{OC} of up to 682 mV and iFF of 80.6% were achieved. Similar results were realized by ion-implanted poly-Si surfaces, herein used as the reference, underlining the high potential of the investigated printing processes

Keywords: Inkjet-printing, Passivating contacts, BC-BJ, TOPCon

1 INTRODUCTION

One promising method to approach the theoretical efficiency limit of silicon solar cells is the integration of passivating contacts [1]. Up to now, increasing the efficiency by improving the bulk lifetime and the dielectric surface passivation of silicon wafers has been extensively studied. Thus, in order to realize solar cells with efficiencies approaching the theoretical limit of 29.43%, passivating contacts are crucial to be developed and practically implemented in photovoltaic devices [2].

Recently, silicon solar cells with tunnel oxide passivated carrier-selective contact (TOPCon) structure [3-10] have demonstrated the high potential and received significant attention. For these types of solar cells, an ultra-thin oxide layer is implemented between a doped polycrystalline silicon (poly-Si) layer and the crystalline silicon (c-Si) wafer to deliver interface passivation of high quality. Efficiently doped poly-Si layers are used to maintain the quasi-fermi level separation in c-Si (high V_{OC}) and to fulfill an efficient majority carrier transport (high FF).

As a result, the conversion efficiency of TOPCon solar cells has been continuously improved up to 25.8% [11, 12], one of the highest efficiencies for crystalline silicon solar cells. A promising route for passivating contacts is their integration into back-contact back-junction (BC-BJ) solar cells indicated by an increase in efficiency of up to 26.1% [9].

As both contacts of BC-BJ solar cells are located at one side of the wafer, the fabrication of such a solar cell requires various patterning steps. Thus, for the formation of local passivating contacts we address printing technology (inkjet-printing) as an industrially relevant or rather scalable method. The technology of choice would enable a fast and easy fabrication of local passivating contacts and, consequently, an industrially attractive approach for high efficiency and low manufacturing costs.

Inkjet-printing in particular is well suited for BC-BJ solar cells as it allows precise consecutive- or simultaneous local printing of boron- (B) and phosphorus- (P) dopant sources in one printing step [13],

whereas dopants can be diffused from the dopant source into the substrate with one single thermal process step ("co-diffusion") [14]. The appeal of this technology lies in its flexibility, precision, digital printing templates, and the non-contact mode. Because of the latter, wafer breakage and contamination during solar cell manufacturing is reduced, which might be of importance at high levels of conversion efficiency.

Focus of this study is to improve and optimize inkjet printing of dopant sources towards higher precision, homogeneity of printed lines and further improvement of lifetime, in order to establish high passivation quality for TOPCon contacts. In this work, printing parameters such as resolution, firing frequency, and pressure waveform (time dependent voltage at piezo) were tuned to develop and optimize inkjet processes for several inks, including three P- and three B dopant inks (B-ink and P-ink).

2 EXPERIMENTAL DETAILS

2.1 Lifetime sample preparation

Symmetric lifetime samples were realized on planar shiny-etched (100) oriented phosphorous-doped *n*-type float-zone (FZ) silicon wafers with a specific resistivity of 1 Ωcm and a thickness of 200 μm . Wafers were cleaned according to the radio corporation of America (RCA) cleaning procedure and an ultra-thin silicon oxide (SiO_x) layer, approximately 1.3 nm, was thermally grown in a tube furnace at 600°C for 10 minutes on both sides. Subsequently, a 50 nm intrinsic amorphous silicon (a-Si(i)) layer was deposited on both sides of the wafer by LPCVD (deposition temperature of 485°C) (Fig. 1). In order to apply dopant sources, B- and P-ink, a *PixDro LP50* inkjet-printer was used. The wafers were dipped in an aqueous solution of 1% hydrofluoric acid (HF) in order to guarantee a clean surface before printing. After printing areas of $A = 30 \times 30 \text{ mm}^2$, the wafers were cured on a hotplate in order to evaporate the organic components at temperatures of $T_{HP} = 300^\circ\text{C}$ for $t_{HP} = 5 \text{ min}$ (B-ink(3)), and $T_{HP} = 200^\circ\text{C}$ for $t_{HP} = 5 \text{ min}$ (for B-ink(1), B-ink(2), and P-ink).

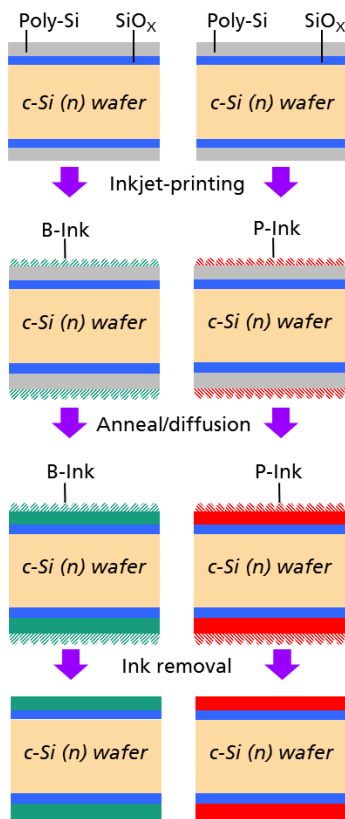


Figure 1: Schematic illustration of the structure of c-Si/SiO_x/poly-Si symmetrical lifetime samples. The SiO_x layer has been grown thermally in a tube furnace and features a layer thickness of about 1.3 nm. The poly-Si has been deposited by means of low pressure chemical vapour deposition (LPCVD) and features a thickness of 50 nm. The doping of the poly-Si layer was realized by inkjet-printing of dopant sources and annealing.

The curing conditions were determined regarding the recommendations of the material suppliers and after performing preliminary experiments. In order to obtain a proper droplet formation and, accordingly, homogeneous layers, the time-dependent piezo-voltage (wave form), firing frequency, or printing resolution were varied.

Afterwards, a high-temperature anneal is performed in a tube furnace under nitrogen atmosphere. The annealing process serves for activation of diffusion processes, as well. Temperature profiles for annealing were evaluated in these experiments with a maximum temperature of $T_p = 900^\circ\text{C}$, 925°C or 950°C and a dwell time of $t_p = 10$ min or 30 min, as listed in Fig. 2. Following the annealing process, residuals were removed in a buffered solution of 10% HF.

2.2 Lifetime sample characterization

After ink removal, the passivation quality on the surface of the symmetrical lifetime samples was measured by means of quasi-steady state photoconductance (QSSPC) measurements through determining the implied open-circuit voltage (iV_{OC}) and the implied fill factor (iFF). These measurements were performed on a WCT-120 lifetime tester from Sinton Instruments [16]. Thereafter, the wafers were subjected to a hydrogenation process in a remote plasma hydrogen passivation (RPHP) system at 400°C for 30 min. The QSSPC measurements were repeated after RPHP in order

to investigate the effect of hydrogenation on passivation quality. The sheet resistance of doped regions was

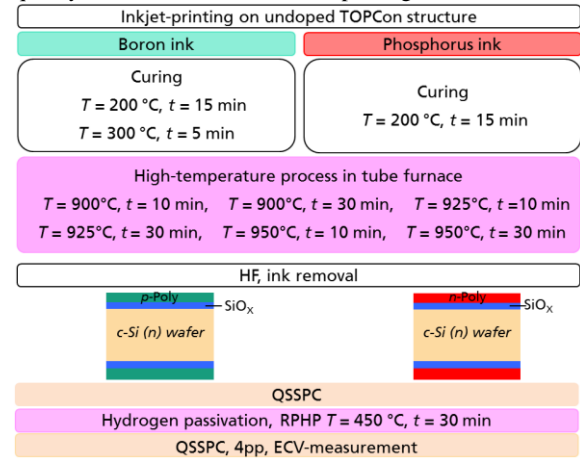


Figure 2: Schematic process sequence for fabrication of lifetime samples. An overview of different groups to investigate influence of the printing and the annealing process on the passivation quality of layers.

determined by a 4-point probe. Subsequently, the doping profile was measured by electrochemical capacitance voltage (ECV) measurements by using a WEP CV21 ECV profiler.

3 RESULTS AND DISCUSSION

3.1 Inkjet-printing process

In order to optimize the jetting performance for B- and P-inks, the integrated high-speed drop-view camera of the PixDro LP50 was utilized to analyze the droplet formation, while varying the jetting settings.

Figure 3 shows a microscopic image of droplets on a shiny-etch surface printed by using a 10 pl print-head and a print resolution in x- and y-direction of 100 dpi. The droplet diameter on the substrate is $33 \mu\text{m}$, hence, very precise while comparing to findings from literature [15]. The improvement has been obtained by optimizing the pressure wave-form and firing frequency.

Figure 4 shows inkjet-printed lines on a shiny-etched surface as realized by using a 10 pl print-head and a resolution of 100 dpi in x- and 700 dpi in y-direction. The image shows a reliable application of lines with very well defined edges. This feature is of great importance especially for manufacturing IBC solar cells.

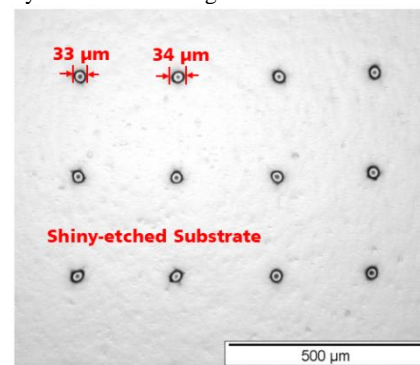


Figure 3: Droplets on a shiny-etched surface printed by using a 10 pl print-head and a resolution in x- and y-direction of 100 dpi. The diameter of droplets is $\sim 33 \mu\text{m}$.

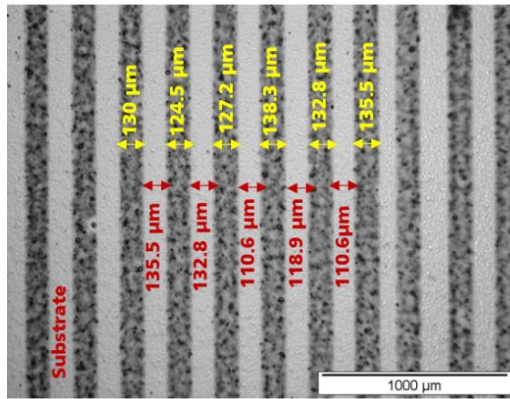


Figure 4: Inkjet-printed lines on a shiny-etched surface using a 10 pl print-head and a resolution of 100 dpi in x- and 700 dpi in y-direction.

3.2 Passivation quality of lifetime samples

In order to investigate the surface passivation quality, the iV_{OC} and iFF values of samples were extracted from injection level dependent lifetime measurements right after the annealing process (before introducing samples to the RPHP). Figure 5 illustrates the iV_{OC} (top) and the iFF (bottom) for P- and B-dopant sources, evaluated for different annealing processes. Open symbols show values measured directly after annealing, and closed symbols represent values after RPHP (H) passivation. All P- and B-doped samples showed an improvement of iV_{OC} and iFF after RPHP.

For P-doped samples, the iV_{OC} improves slightly by increasing the anneal temperature from 925°C to 950°C (Fig. 6). At 950°C, increasing annealing time from 10 min to 30 min results in a reduction in iV_{OC} of all samples. However, the iV_{OC} of P-ink(3) doped samples does not degrade after performing RPHP. The P-ink(2) and P-ink(3) exhibited a high iV_{OC} of up to 733 mV. With ion-implantation 732 mV could be achieved [15]. With the same inks, a high iFF of up to 86.5% and 86.4% were achieved, respectively. With Ion-Implantation 87.3% could be obtained [15]. With B-ink dopant sources, an iV_{OC} of up to 682 mV and an iFF of 80.6% were achieved (B-ink(3)). Although promising, the B-inks are not well developed as the P-inks, yet.

Figure 6(left) shows the phosphorous profiles of doped samples by P-ink(3) measured by ECV profiling from poly- to the c-Si. It can be clearly seen from the profiles that annealing for 30 min at 950°C is too long, which causes excessive diffusion of phosphorus and, thus, very deep profiles. The sheet resistance of 302 Ω/sq and 107 Ω/sq was calculated from profiles of samples annealed at 950°C for 10 min and 30 min, respectively. Figure 7(right) illustrates boron profiles measured by ECV profiling. The doping profiles of B-ink(2) samples indicate that annealing conditions of 925°C, 30 min lead to excessive diffusion of boron enabling a very deep profile especially inside the c-Si. The calculated sheet resistance of the profile of B-ink samples annealed at 900°C, 30 min, 925°C, 10 min, and 925°C, 30 min are respectively, 222 Ω/sq, 137 Ω/sq and 277 Ω/sq. These values were confirmed by a 4-point probe measurement.

3.3 Simulation results

Experimental results of the best samples were used as input parameters for simulation of BC-BJ solar cell devices by Quokka. For this simulation, a 200 μm thick base with resistivity of 1 Ωcm were considered. The contact resistivity (ρ_C) of B- and P-doped layers has not been determined, yet. Thus, we assumed relatively low values of ρ_C , and as a result the FF is rather low. The following additional assumptions for simulation are shown in Table I.

Table I. Assumptions were used as the input for simulation of an BC-BJ cell by Quokka

Input parameters	Value
Sheet resistance of emitter	200 Ω/cm ²
J_0 of emitter	50 fA/cm ²
Contact resistivity of emitter ($\rho_{C,emitter}$)	10 mΩ cm ²
Sheet resistance of back surface field (BSF)	140 Ω/sq
J_0 of BSF	3 fA/cm ²
Contact resistivity of BSF ($\rho_{C,BSF}$)	10 mΩ cm ²
Pitch width (x_{pitch})	500 μm
Emitter width ($x_{emitter}$)	360 μm
Gap width (x_{gap})	20 μm
BSF width (x_{BSF})	100 μm

Based on the assumptions (Table 1), $V_{OC} = 707$ mV, $J_{SC} = 42.8$ mA/cm², $FF = 80.2\%$, and $\eta = 24.3\%$ were obtained, which is promising. The relatively low V_{OC} can be explained by rather low carrier life time of the B-doped layers. Thus improving passivation quality of the B-doped layers, especially by improving the formulation of B-inks is necessary.

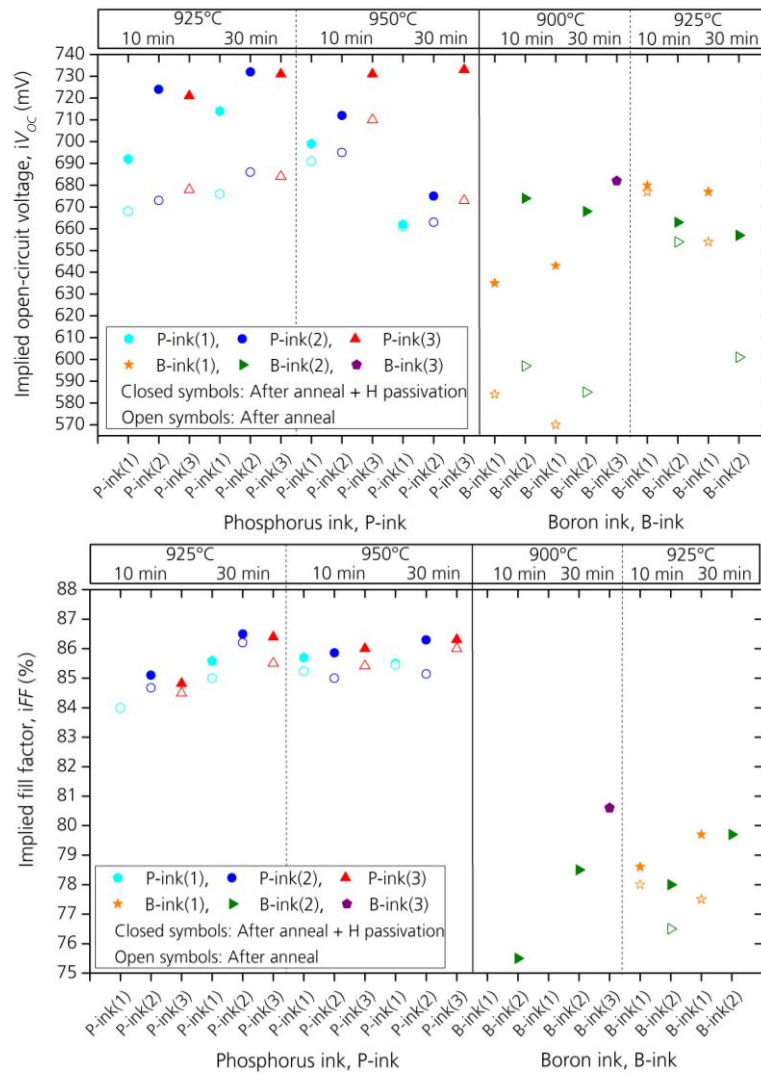


Figure 5: The implied open-circuit voltage (iV_{oc}) (top) and the implied fill factor (iFF) (bottom) for P- and B-dopant sources, evaluated for different high-temperature processes. Open symbols show values measured directly after annealing, and closed symbols represent values after RPHP (H) passivation.

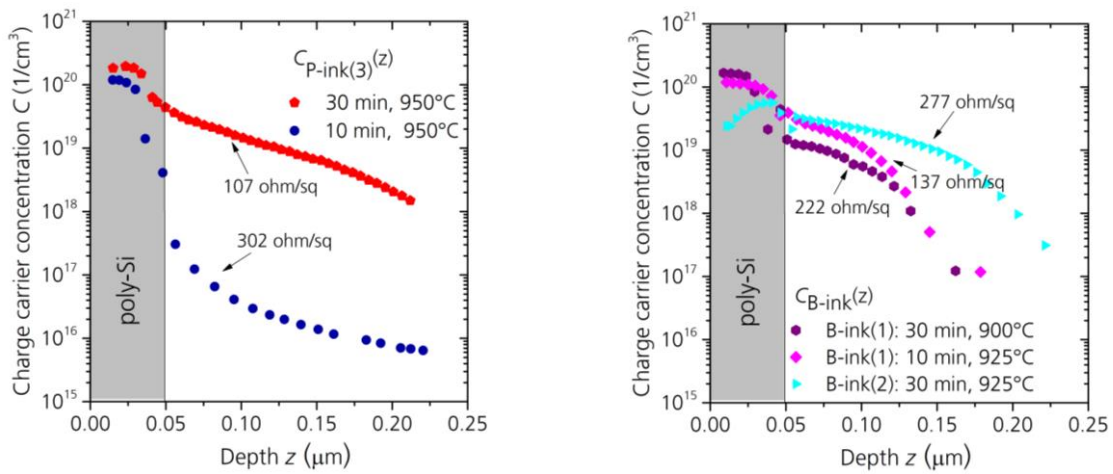


Figure 6: Charge carrier concentration vs. depth for selected samples doped by P-ink(3), annealed at 950°C for 10 and 30 min (left), and doped by B-ink(1) and B-ink(2), annealed at 900°C and 925°C (right).

4 SUMMARY AND CONCLUSION

The printing of phosphorus and boron dopant sources for poly-Si/SiO_x/c-Si passivating contacts were studied and improved. It was observed that the excellent passivation quality can be achieved by inkjet-printing of phosphorus inks with $iV_{OC} = 733$ mV and $iFF = 86.4\%$. Variation of iV_{OC} and iFF with annealing temperature and time reveal that 925°C and 30 min is an optimum temperature and time for most of the evaluated phosphorus inks. Inkjet-printing of boron inks enables the formation of local passivating contacts with $iV_{OC} = 682$ mV and $iFF = 80.6\%$. Further research needs to be done on ink formulation in order to increase the passivation quality. The lowest sheet resistances of B-doped layers were measured to be 200 Ω/sq (Four-Point Probe) for samples annealed at 900°C and 30 min. Results of the best samples were used as an input for a simulation by Quokka. $V_{OC} = 707$ mV, $J_{SC} = 42.8$ mA/cm², $FF = 80.2\%$, and $\eta = 24.3\%$ were simulated with an BC-BJ model, which is promising. The relatively low V_{OC} can be explained by the relatively low passivation quality of the B-doped surfaces. Thus improving passivation quality of the B-doped surfaces, specifically by improving the formulation of B-inks or utilization of alternatives is necessary.

ACKNOWLEDGEMENTS

The authors would like to thank anyone involved in this work, the research teams at Fraunhofer ISE PV-TEC and clean room facilities.

This work was funded by the German Federal Ministry for Economic Affairs and Energy within the research project "IMPACT" under contract number 354066.

6 REFERENCES

- [1] R. M. Swanson, "Approaching the 29% limit efficiency of silicon solar cells," in *31st IEEE Photovolt. Specialists Conference (IEEPPVSC)*, pp. 889-894, 2005.
- [2] A. Richter, M. Hermle, S. W. Glunz, "Reassessment of the limiting efficiency for crystalline silicon solar cells," *IEEE J. Photovolt.*, vol.3, no. 4, pp. 1184-1191, 2013.
- [3] F. Feldmann, M. Bivour, C. Reichel, M. Hermle, S. W. Glunz, "A passivated rear contact for high-efficiency n-type silicon solar cells enabling high Vocs and FF > 82%," in *28th European PV Solar Energy Conference and Exhibition (EUPVSEC)*, pp. 988-992, 2013.
- [4] F. Feldmann, M. Bivour, C. Reichel, M. Hermle, S.W. Glunz, "Passivated rear contacts for high-efficiency n-type Si solar cells providing high interface passivation quality and excellent transport characteristics," *Sol. Energy Mater. Sol. Cells.*, vol. 120, pp. 270-274, 2014.
- [5] F. Feldmann, M. Bivour, C. Reichel, H. Steinkemper, M. Hermle, S.W. Glunz, "Tunnel oxide passivated contacts as an alternative to partial rear contacts," *Sol. Energy Mater. Sol. Cells.*, vol.131, pp. 46-50, 2014.
- [6] F. Feldmann, M. Simon, M. Bivour, C. Reichel, M. Hermle, S.W. Glunz, "Efficient carrier-selective p-and n-contacts for Si solar cells," *Sol. Energy Mater. Sol. Cells.*, vol.131, pp. 100-106, 2014.
- [7] C. Reichel, F. Feldmann, R. Müller, A. Moldovan, M. Hermle, S. W. Glunz, "Interdigitated back contact silicon solar cells with tunnel oxide passivated contacts formed by ion implantation," in *29th European PV Solar Energy Conference and Exhibition (EUPVSEC)*, pp.487-491, 2014.
- [8] D. Yan, A. Cuevas, Y. Wan, J. Bullock, "Passivating contacts for silicon solar cells based on boron-diffused recrystallized amorphous silicon and thin dielectric interlayers," *Sol. Energy Mater. Sol. Cells.*, vol. 152, pp. 73-79, 2016.
- [9] F. Haase, C. Hollemann, S. Schäfer, A. Merkle, M. Reinäcker, J. Krügener, R. Brendel, R. Peibst, "Laser contact openings for local poly-Si-metal contacts enabling 26.1%-efficient POLO-IBC solar cells," *Sol. Energ. Mat. Sol.*, vol. 186, 2018.
- [10] U. Römer, R. Peibst, T. Ohrdes, B. Lim, J. Krügener, T. Wietler, R. Brendel, "Ion implantation for poly-Si passivated back-junction back-contact solar cells," *IEEE J. Photovolt.*, vol.5, pp. 507-514, 2015.
- [11] A. Richter, J. Benick, R. Müller, F. Feldmann, C. Reichel, M. Hermle, S. W. Glunz, "Tunnel oxide passivating electron contacts as full-area rear emitter of high-efficiency p-type silicon solar cells," *Progs. Photovoltaics.*, vol. 26, 2017.
- [12] M. A. Green, Y. Hishikawa, E. D. Dunlop, D. H. Levi, J. H-Ebinger, A. W. Y. Ho-Baillie, "Solar efficiency tables (version51)," *Prog. Photovolt. Res. Appl.*, vol. 26, 2018.
- [13] F. Haase, B. Lim, A. Merkle, T. Dullweber, R. Brendel, C. Günther, M. H. Holthausen, C. Mader, O. Wunnicke, R. Peibst, "Printable liquid silicon for local doping of solar cells," *Sol. Energ. Mat. Sol.*, vol. 179, pp. 129-135, 2018.
- [14] R. Keding, D. Stüwe, M. Kamp, C. Reichel, A. Wolf, R. Woehl, D. Borchert, H. Reinecke, and D. Biro, "Co-diffused back-contact back-junction silicon solar cells without gap regions," *IEEE J. Photovolt.*, vol.3, pp. 1236-1242, 2013.
- [15] Z. Kiaee, C. Reichel, F. Feldmann, M. Jahn, J. D. Huyeng, R. Keding, M. Hermle, F. Clement, "Printed dopant sources for locally-doped SiO_x/poly-Si passivating contacts," in *35th European PV Solar Energy Conference and Exhibition (EUPVSEC)*, pp.792-797, 2018.
- [16] R. A. Sinton, A. Cuevas, "Contactless determination of current-voltage characteristics and minority-carrier lifetime for quasi-steady-state photconductance data," *Appl. Phys. Lett.*, vol. 69, no, 17, pp. 2510-2512, 1996.